APPLICATION NOTE

Advancing Autophagy Detection: HTRF LC3B-II Assay for Specific and Reliable LC3B-II detection.

Authors

Sonia Brun,
Eric Malaud,
Stéphane Martinez &
Fabienne Charrier-Savournin
Revvity, Inc.

Introduction

Autophagy is an evolutionary conserved cellular process that occurs in all eukaryotic cells, ranging from yeast to mammals. Autophagy plays a pivotal role in maintaining cellular homeostasis for degrading and recycling cellular components such as misfolded or aggregated proteins, or damaged mitochondria. Autophagy is also involved in the cellular response to various cellular stresses such as nutrient deprivation, hypoxia, or pathogens infection (Klionsky et al., 2021; He et al., 2009).

The canonical pathway of autophagy involves a series of orchestrated steps, starting with the formation of a double-membraned structure called the phagophore, as featured Figure 1 (Feng et al., 2014). This membrane elongates and engulfs cytoplasmic cargo, ranging from damaged organelles to protein aggregates. Key players in autophagy regulation include the autophagy related (ATG) proteins, which coordinate the different stages of autophagosome formation, maturation, and fusion with lysosomes (Mizushima et al., 2011). Initiation of autophagy often relies on the activation of the ULK1 complex, which responds to nutrient and energy status. As cellular stressors accumulate, signaling pathways such as mTORC1 are inhibited, triggering autophagy induction (Russell et al., 2013).

During elongation and closure of the autophagosome, lipidation of microtubule-associated proteins 1A/1B light chain 3B (hereafter referred to as LC3) is crucial for cargo recruitment. Indeed, the cytosolic form of LC3 (LC3-I) is converted to a phosphatidylethanolamine (PE) LC3 conjugate (LC3-PE or LC3-II) which is specifically associated with autophagosomal membranes (Kabeya et al., 2000). The cargo-loaded autophagosomes eventually fuse with lysosomes, forming autolysosomes where lysosomal hydrolases degrade the

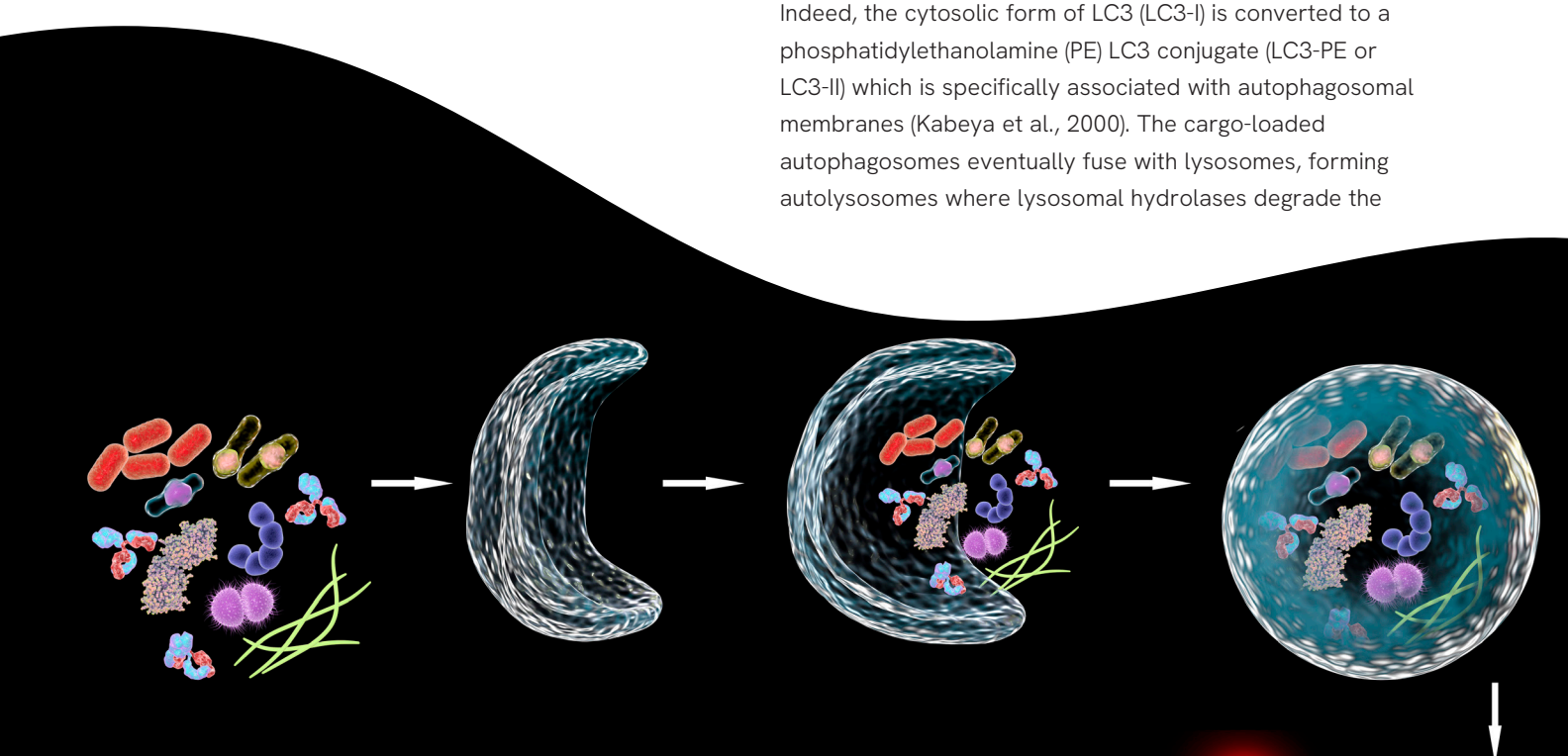

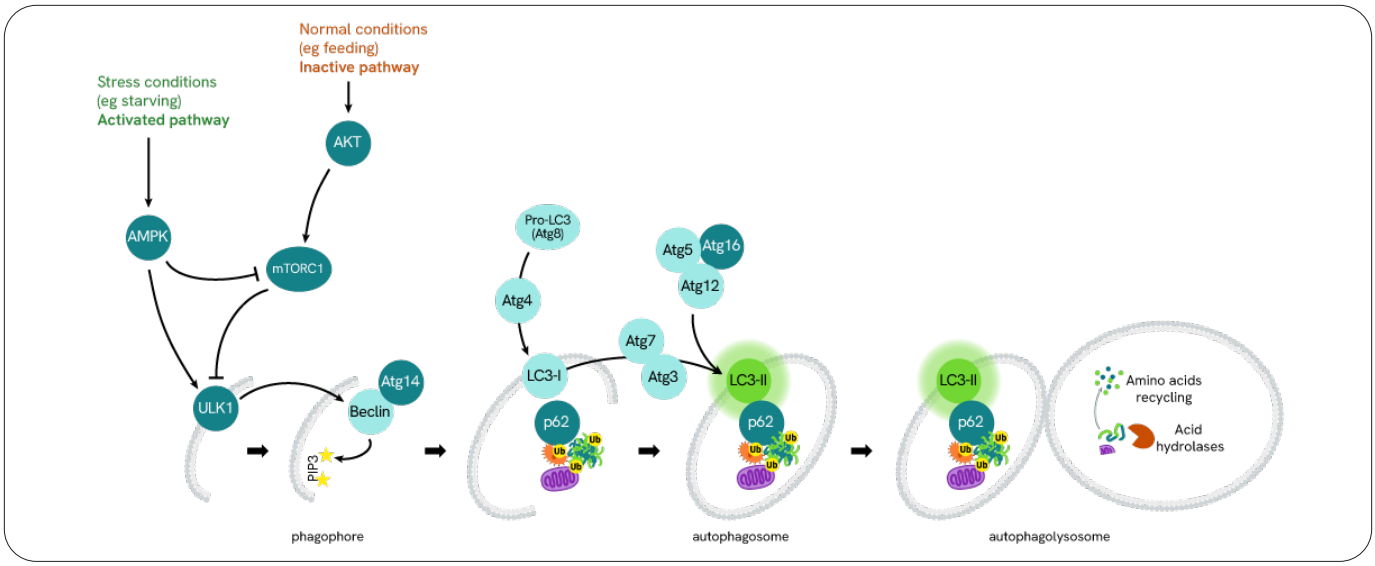

Figure1: Simplified pathway of autophagy

engulfed contents including LC3-II (Yang and Klionsky, 2010; Agrotis et al., 2019). This degradation process generates recycled biomolecules that can be utilized for energy production or biosynthesis, thereby sustaining cellular viability during stress.

Dysregulation of autophagy has been implicated in various diseases, including neurodegenerative disorders, cancer, and metabolic conditions (Levine et al., 2008; Morel et al., 2017; Klionsky et al., 2021; Debnath et al., 2023; Bestion et al., 2023).

Understanding the mechanisms of autophagy regulation offers promising avenues for therapeutic interventions aimed at restoring cellular balance and combating disease pathology.

Studying the molecular basis of autophagy involves a variety of techniques, which have evolved over time. Western blotting is often used to detect and quantify specific proteins involved in autophagy, by using antibodies against key autophagy-related proteins such as LC3 or p62/SQSTM1. Immunofluorescence microscopy and fluorescence-based assays allow to visualize the subcellular localization and quantify the expression level of endogenous or fluorescent tagged proteins (e.g., GFP-LC3). Genetic manipulation of ATG genes using RNA interference or CRISPR/Cas9 gene editing can provide insights into the roles of specific genes and pathways in regulating autophagy.

Knockdown or knockout of key autophagy genes can elucidate their functions and reveal how they contribute to the molecular mechanisms underlying autophagy.

These techniques, used alone or in combination, enable researchers to dissect the molecular basis of autophagy and uncover the intricate regulatory networks that govern this essential cellular process.

Herein, we describe a detailed and comprehensive validation study of an innovative HTRF LC3B-II immunoassay. To this end, HTRF results were compared to the standard LC3 Western Blot used as a reference method, as depicted in the Figure 2. In addition, a panel of wild type (WT), siRNA transfected, as well as Knockout ATG HAP1 cells were included as relevant cellular models. The HTRF LC3B-II assay demonstrated high specificity and sensitivity for detecting LC3B-II, the lipidated form of LC3 involved in autophagosome formation. Quantitative analysis revealed a strong correlation between HTRF signals and LC3-II levels determined by Western blotting across a range of cell types and experimental conditions. Importantly, the HTRF LC3B-II assay was able to detect subtle changes in autophagic flux induced by pharmacological treatment, highlighting highly reliable and precise assay features for studying dynamic alterations in autophagy. Overall, our validation study demonstrates that the HTRF LC3B-II immunoassay represents a robust and reliable tool for quantifying autophagy in diverse cellular contexts, offering advantages in terms of speed, throughput, and precision compared to traditional Western Blot method.

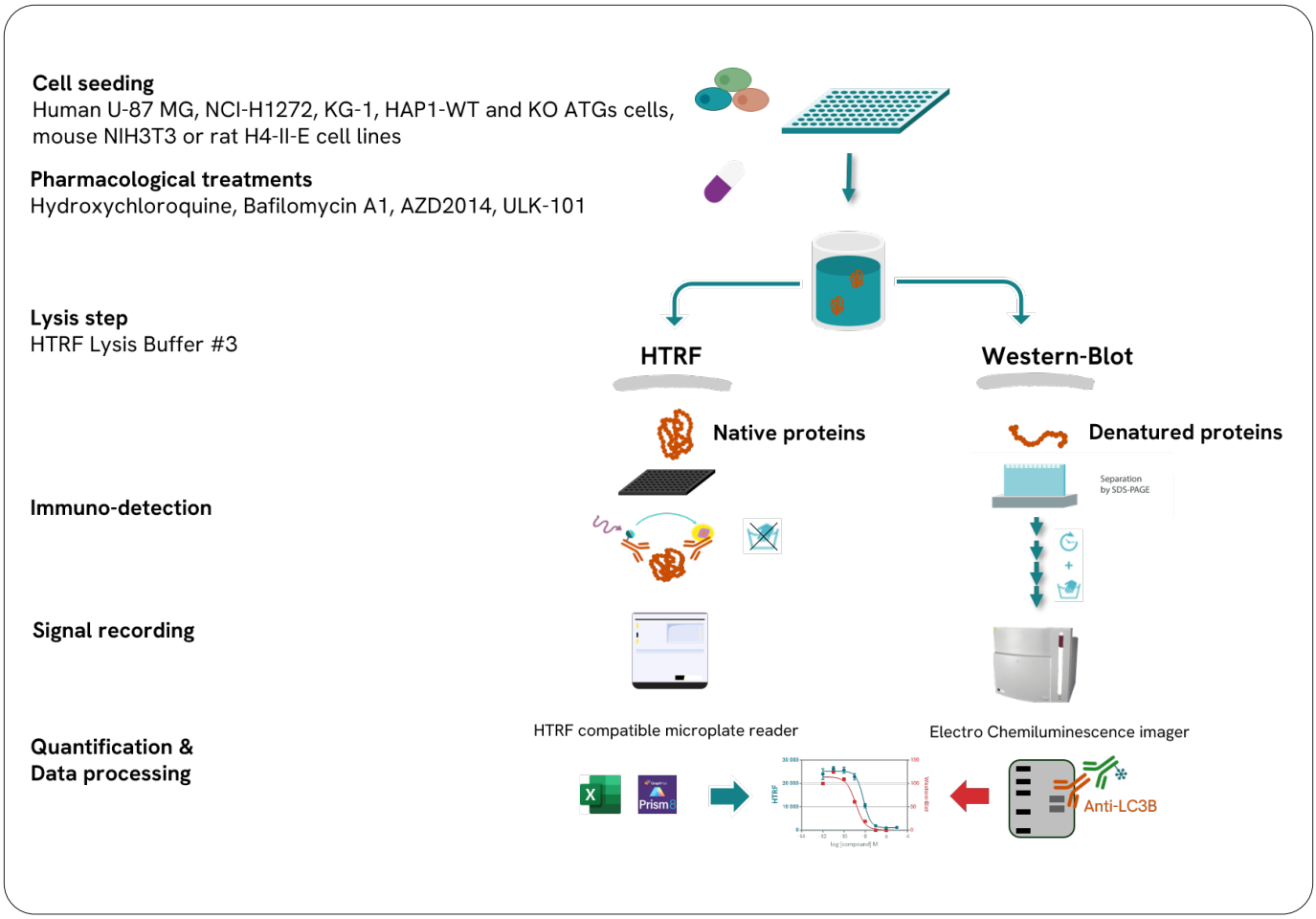

Figure 2: Workflow of the study design

Results

Comparison of HTRF LC3B-II detection kit and Western Blot analysis

U-87 MG cells were seeded at a density of 25,000 cells per well in a 96-well culture-treated plate and treated with increasing concentrations of Hydroxychloroquine (HCQ) for 4 hours, a widely recognized late-stage autophagic flux inhibitor (Rebecca et al., 2019). Following cell lysis using HTRF Lysis Buffer 3, equal amounts of lysates were subjected to analysis using both HTRF and Western Blot techniques. HTRF and chemiluminescent signals were normalized using GAPDH housekeeping protein, employing the HTRF Housekeeping GAPDH kit and GAPDH immunoblotting.

As illustrated in Figure 3, the results from HTRF LC3B-II and Western Blot analyses exhibit a high degree of correlation, indicating the comparability of these two methods and the consistency of HTRF results.

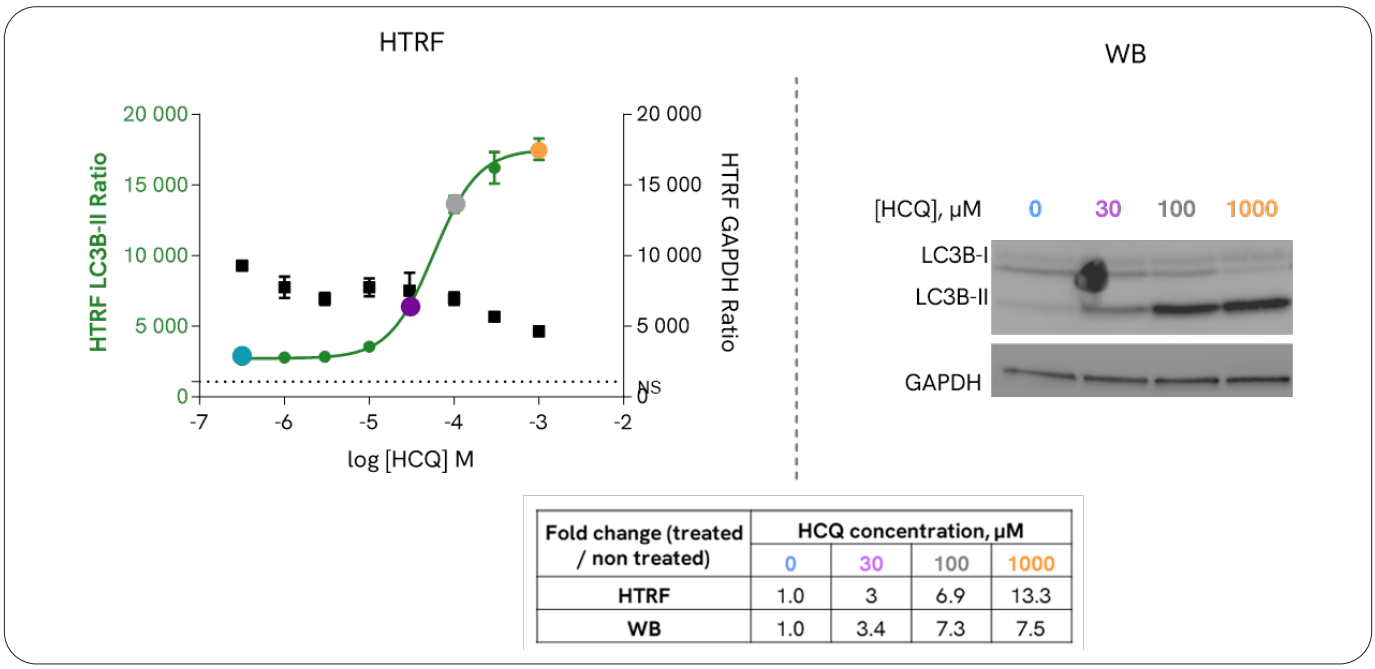

Fold change (treated / non treated)	HCQ concentration, µM			
	0	30	100	1000
HTRF	1.0	3	6.9	13.3
WB	1.0	3.4	7.3	7.5

Figure 3: Correlation between HTRF LC3B-II and the Western-Blot detection methods. The fold change represents the LC3B-II normalized signal in treated conditions compared to untreated conditions.

Selective detection of LC3B isoform using HTRF

In mammalian cells, the LC3 protein family comprises multiple isoforms (LC3A, LC3B, LC3B2, and LC3C), each exhibiting distinct tissue distributions and poorly understood functions (Klionsky et al., 2021).

NCI-H1272 cells (seeded at 10,000 cells per well in a 96-well culture-treated plate) were transfected with ON-TARGETplus SMARTPool siRNAs targeting LC3A, LC3B, and LC3C isoforms, along with a non-targeting siRNA serving as a negative control. Following a 24-hour incubation, cells were replenished with fresh culture medium and further incubated for an additional 24 hours. Subsequently, cells were treated with 2.5 µM AZD2014, a well-known mTOR inhibitor, and 100 nM Bafilomycin A1 (BafA1), a vacuolar H (+)- ATPase inhibitor, for 4 hours inhibitor (Bensalem et al., 2021, Klionsky et al., 2021). Cell lysates were then analyzed using the HTRF LC3B-II kit.

As depicted in Figure 4, knockdown of the LC3B isoform via siRNA transfection resulted in a nearly complete loss of HTRF signal induced by co-treatment with AZD2014 and BafA1. In contrast, knockdown of LC3A and LC3C genes did not lead to any significant modulation of the signal. These findings provide compelling evidence that the HTRF detection antibodies specifically recognize the LC3B isoform and do not cross-react with other LC3 isoforms.

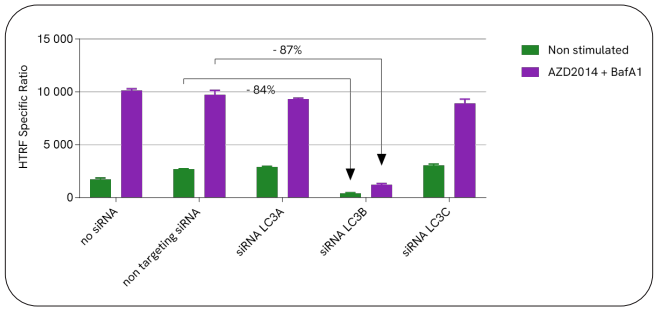

Figure 4: Selective detection of LC3B isoform using HTRF LC3B-II detection kit

Specific detection of LC3B-phosphatidylethanolamine conjugate (LC3B-II) using the HTRF LC3B-II detection kit

Immediately following synthesis, nascent LC3 (pro-LC3) undergoes processing by the cysteine protease Atg4B, leading to the formation of LC3-I. This priming/activation step exposes a specific glycine residue, enabling Atg7 and Atg3 to conjugate LC3-I to PE, forming LC3-II. LC3-II is integrated into both the inner and outer membranes of autophagosomes during autophagosome biogenesis, facilitated by the Atg5/Atg12/Atg16L complex. At the conclusion of the autophagy pathway, intra-autophagosomal components undergo degradation by lysosomal hydrolases, with degradation products subsequently recycled back into the cytosol. Simultaneously, the PE group of LC3-II is removed by Atg4B, allowing for the recycling of LC3-I

(Agrotis et al., 2019). Consequently, two forms of LC3 coexist within cells: cytosolic LC3-I and PE-conjugated LC3-II, predominantly found on isolation membranes and autophagosomes, with lesser presence on autolysosomes (Mizushima et al., 2007).

Given that LC3-II levels correlate with the abundance of autophagosomes, it serves as the primary biochemical marker for autophagy. Therefore, the specific detection of LC3B-II, rather than LC3B-I, is crucial for monitoring autophagy and related processes. To validate the specificity of our HTRF assay for detecting LC3B-II, we utilized various HAP1 knockout (KO) cell lines with distinct LC3B expression patterns: HAP1 parental (referred to as HAP1 WT), containing both LC3B-I and LC3B-II; HAP1 KO Atg7, harboring only the LC3B-I form; and HAP1 KO Atg4B, possessing pro-LC3B exclusively. Additionally, HAP1 KO LC3B cells lacking LC3B were employed as a negative control. LC3B immunoblotting results presented in Figure 5B confirmed these LC3B expression patterns, consistent with literature findings (Wang et al., 2013). Subsequently, various HAP1 cell lines (seeded at 25,000 cells per well in a 96-well culture-treated plate) were treated with HCQ for 4 hours, and cell lysates were subjected to analysis using the HTRF LC3B-II kit.

As depicted in Figure 5A, HTRF signal was exclusively detected in the HAP1 WT cell line, with basal signal levels increasing following HCQ treatment, consistent with literature observations (Rebecca et al., 2019). Conversely, near-background signals were observed in HAP1 KO Atg4B and Atg7 cells, as well as in the negative control (HAP1 KO LC3B). Thus, we conclude that our assay enables specific detection of LC3B-II, distinguishing it from LC3B-I.

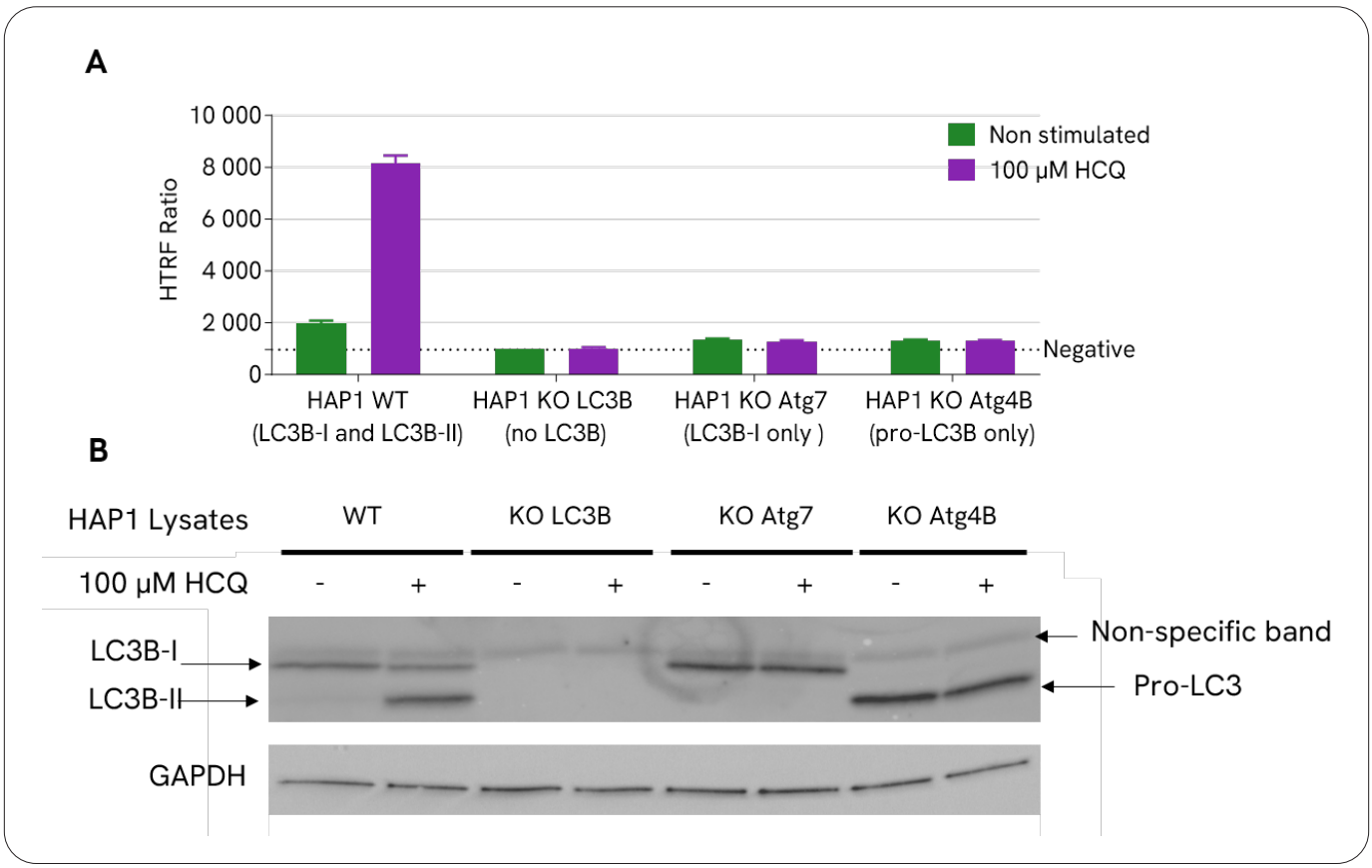

Figure 5: LC3B-II detection in several HAP1 knockout (KO) cell lines using both the HTRF LC3B-II Kit (Panel A) and LC3B immunoblotting (Panel B) methods.

Assessment of LC3B-I influence on LC3B-II detection using HTRF

To evaluate the impact of LC3B-I presence on LC3B-II detection, we designed experiments to manipulate the LC3-II/LC3-I ratios. Samples were prepared by combining a predominantly LC3B-II-containing sample from HCQ-treated HAP1 WT cells with increasing amounts (ranging from +25% to 100% v/v) of a sample containing only LC3B-I from HAP1 KO Atg7 cells. Additionally, positive and negative controls were included: HCQ-treated HAP1 WT sample and LC3B-deficient HAP1 KO Atg4B sample, respectively. The reference signal was established using the HCQ-treated HAP1 WT sample mixed with lysis buffer.

Figure 6A demonstrates that the HTRF signal for samples combining HCQ-treated HAP1 WT sample with different quantities of LC3B-I-containing sample remained consistent with the reference signal, indicating that LC3B-I presence did not affect LC3B-II detection. Similar results were observed for the negative control (LC3B-deficient HAP1 KO Atg4B sample) (data not shown). Conversely, the addition of HCQ-treated HAP1 WT sample led to a dose-dependent increase in HTRF signal (purple bars). LC3B immunoblotting results in Figure 6B validated these observed LC3B expression patterns.

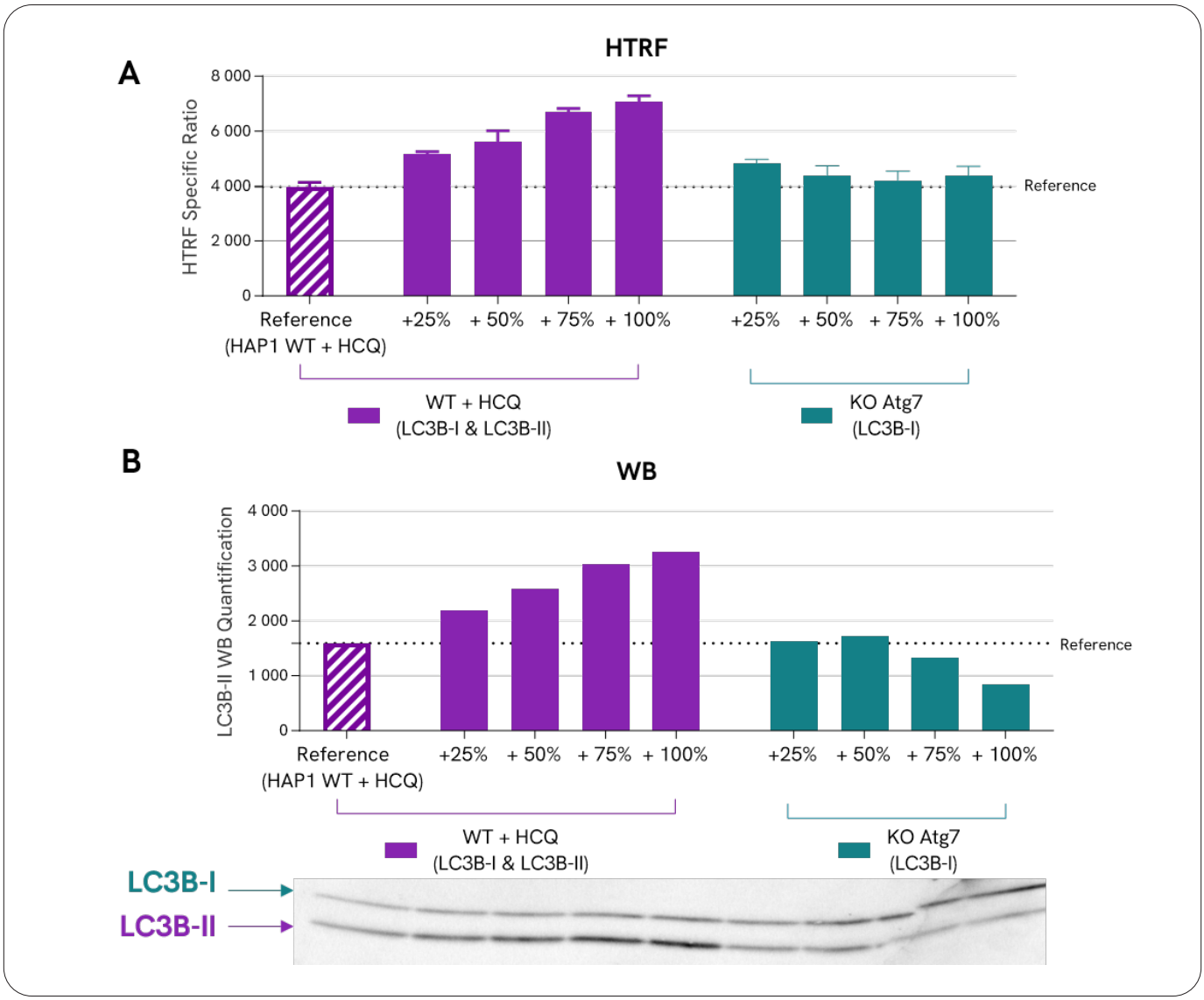

Figure 6: LC3B-II detection using both the HTRF LC3B-II Kit (Panel A) and LC3B immunoblotting (Panel B) methods. The samples were prepared by mixing a sample primarily containing LC3B-II (from HCQ-treated HAP1 WT cells) with various quantities of either a sample predominantly containing LC3B-II (HCQ-treated HAP1 WT cells, positive control, purple bars) or a sample containing only LC3B-I (from HAP1 KO Atg7 cells, blue bars). The reference signal (purple hatched bar) was obtained by mixing the HCQ-treated HAP1 WT sample with lysis buffer.

Further manipulation of the LC3B-II/LC3B-I ratios, as described in Figure 7A, confirmed these findings. A dose-dependent increase in signal was observed for samples combining the LC3B-I-containing sample with various amounts of the LC3B-II-rich sample (purple bars).

However, the addition of the LC3B-I-containing sample alone (blue bars) and the LC3B-deficient sample (data not shown) had no impact on the HTRF signal.

These results collectively validate that LC3B-I presence does not interfere with LC3B-II detection using our HTRF kit.

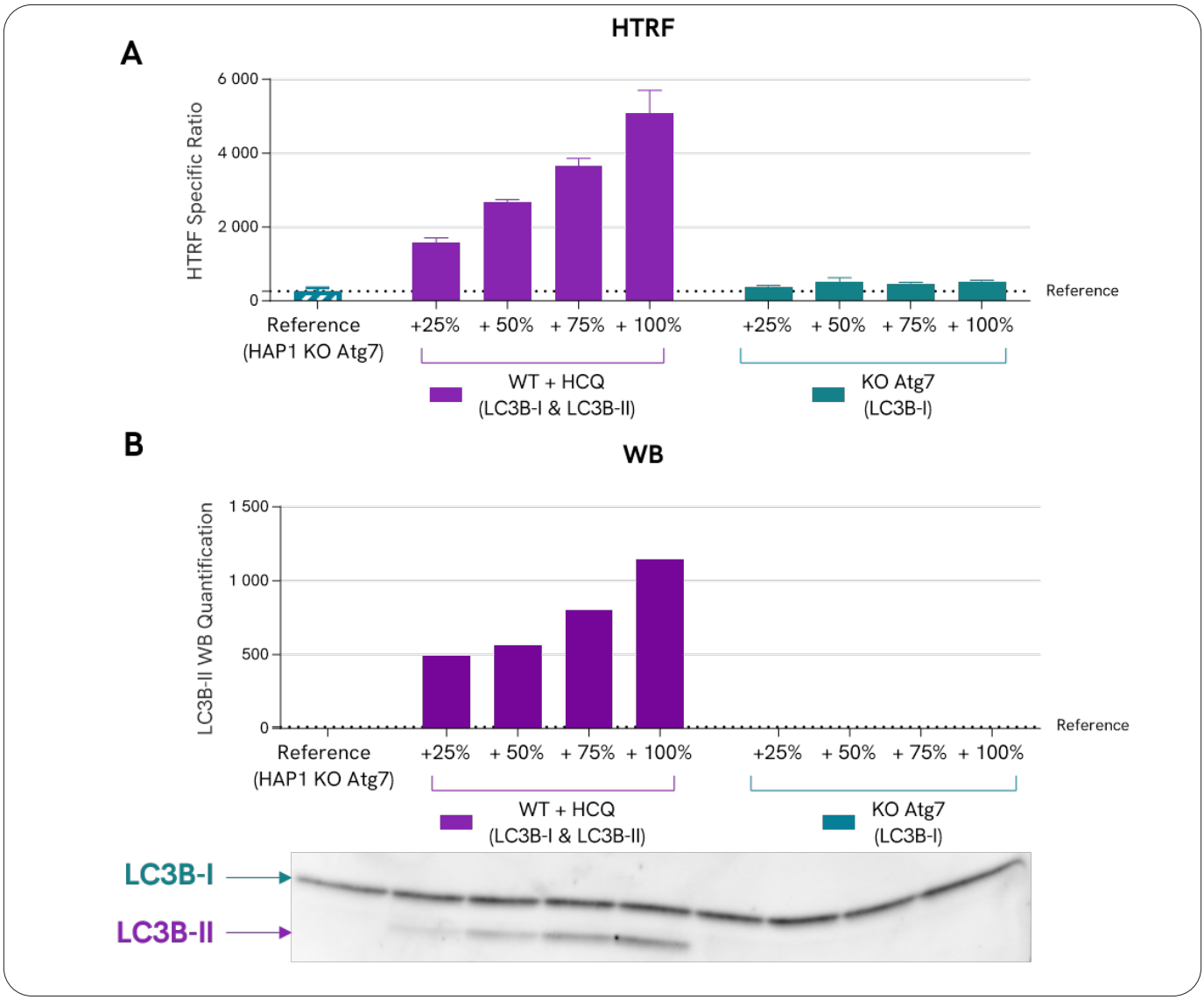

Figure 7: LC3B-II detection using both the HTRF LC3B-II Kit (Panel A) and LC3B immunoblotting (Panel B) methods. The samples were prepared by mixing a sample containing only LC3B-I with varying amounts of a sample primarily containing LC3B-II (HCQ-treated HAP1 WT cells, purple bars) or a sample containing only LC3B-I (HAP1 KO Atg7 cells, blue bars). The reference signal (blue hatched bar) was obtained by mixing the LC3B-I-only sample with lysis buffer.

Pharmacological validation of HTRF LC3B-II assay in U-87 MG cells

We conducted pharmacological validations of our HTRF LC3B-II assay using various autophagy modulators in U-87 MG cells:

1. Induction of autophagy with AZD2014, a mTOR inhibitor (Figure 8A)
2. Inhibition of autophagic flux with BafA1 (Figure 8B)
3. Decrease of AZD2014-induced autophagy with ULK-101, an ULK1/2 inhibitor (Figure 8C)

These results are in accordance with literature findings (Yamamoto et al., 1998; Bensalem et al., 2021; Martin et al., 2018), providing robust pharmacological validation of our HTRF LC3B-II assay.

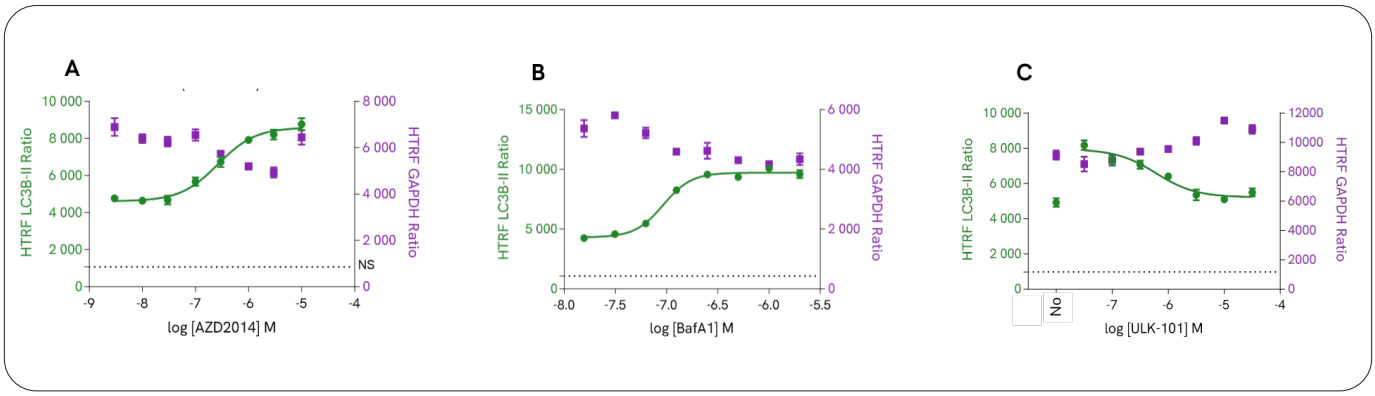

Figure 8: LC3B-II detection in U-87 MG cells treated with AZD2014 (panel A) or BafA1 (panel B), as well as cells co-treated with AZD214 and ULK-101 (panel C), utilizing the HTRF LC3B-II Kit

Distinguishing autophagy activators from autophagic flux inhibitors using LC3-II levels

Both autophagy activators and autophagic flux inhibitors can lead to increased levels of LC3-II and the accumulation of autophagosomes. Therefore, comparing LC3-II levels between treatments with or without a late-stage autophagy inhibitor, such as Baf A1, is a common method to characterize new autophagy modulators and differentiate between autophagy activators and autophagic flux inhibitors (Mizushima et al., 2007; Klionsky et al., 2021).

An additive effect on LC3-II levels in the presence of BafA1 indicates that the treatment enhances autophagic flux, as demonstrated in Figure 9A for AZD2014. Conversely, no difference in LC3-II levels in the presence of BafA1 compared to treatment alone suggests a complete block in autophagy at the terminal stages, as depicted in Figure 9B for HCQ).

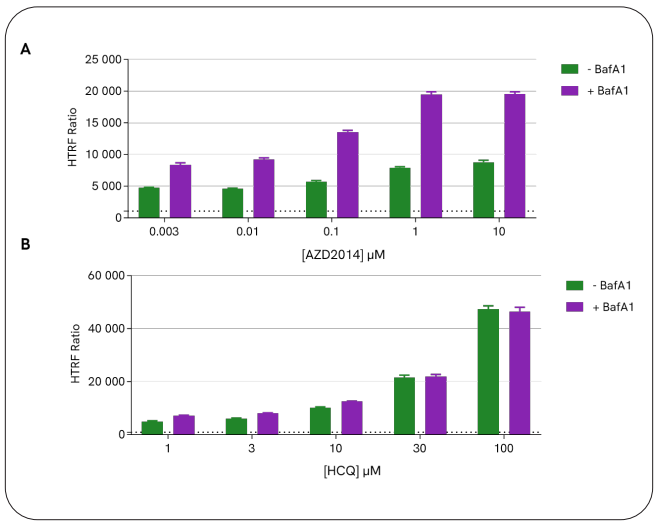

Figure 9: LC3B-II detection in U-87 MG cells treated with AZD2014 (panel A), or HCQ (panel B) in the presence or absence of Baf A1 using the HTRF LC3B-II Kit

Characterization of HTRF LC3B-II assay in adherent and suspension cell lines from human, mouse, and rat

To comprehensively assess the performance of our HTRF LC3B-II assay, we examined various cell densities across adherent and suspension cell lines from human, mouse, and rat origins (Figure 10). The assay consistently exhibited significant positive signals across all tested conditions and cell lines, indicating its ability to detect LC3B-II protein efficiently in both adherent (Figure 10A) and suspension (Figure 10B) cell cultures. Moreover, our assay demonstrated cross-reactivity with mouse (Figure 10C) and rat (Figure 10D) LC3B-II proteins. These findings underscore the versatility and translational potential of our assay for research applications.

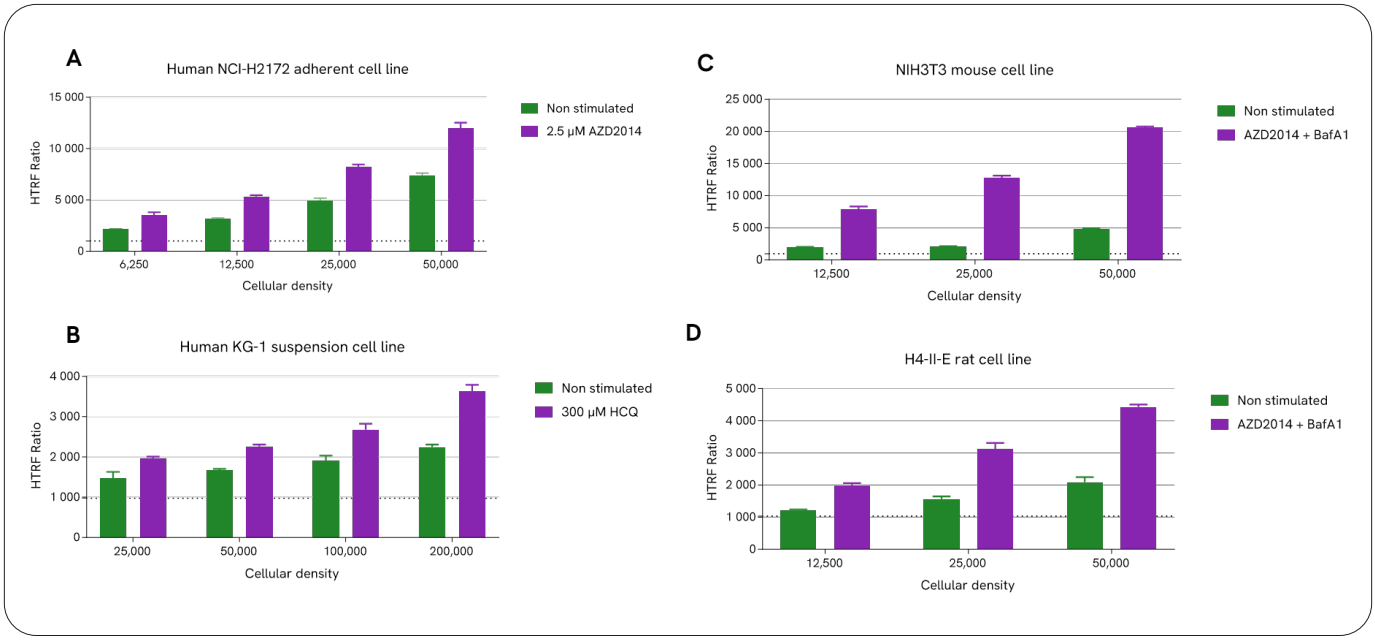

Figure 10: LC3B-II detection in NCI-H2172 human adherent cells treated by AZD2014 (panel A), KG-1 human suspension cells treated by HCQ (panel B), NIH/3T3 mouse cell line (panel C) or H-4-II-E rat cell line (panel D) co-treated by 2.5 µM AZD2014 and 100 µM BafA1 (panel C) using the HTRF LC3B-II Kit

Conclusion

Revvity's HTRF LC3B-II kit offers a user-friendly, no-wash, add-and-read protocol that delivers accurate and reliable results as shown in existing literature. The validations conducted demonstrate its sensitivity, specificity for the LC3B-II isoform, versatility across human, mouse, and rat cells, and strong correlation with Western Blot, a standard technique.

This kit is rapid, homogeneous, and easily automated, enabling miniaturization and streamlined assay development. It serves a wide range of applications, including basic and translational research, target discovery and validation, high-throughput screening (HTS), primary and secondary screening, and lead optimization.

Importantly, Revvity's HTRF LC3B-II kit stands out as the first immunoassay capable of specifically detecting the LC3-II form without requiring any pre-analytical treatment. Along with Revvity's related autophagy /mitophagy detection kits such as p62SQSTM1, ATG14, ATG16L1, ULK1 or TOM20, the addition of HTRF LC3B-II kit provides a comprehensive no-wash platform to unravel autophagy molecular mechanisms.

Materials and reagents

	Reagent	Supplier	Part Number
Microplates	SpectraPlate 96-well, clear, tissue-culture treated, with lids	Revvity	6005650
	ProxiPlate 384-shallow well Plus, white	Revvity	6008280/9
	AlphaPlate 384-well, light gray, untreated	Revvity	6005350/9
HTRF kits	HTRF (h/m) LC3B II Kit	Revvity	64LC3B2PEG/H
	HTRF GAPDH Housekeeping Cellular Kit	Revvity	64GAPDHPEG/H
siRNA	ON-TARGETplus Human MAP1LC3A siRNA	Revvity	L-013579-00-0005/0010/0020/0050
	ON-TARGETplus Human MAP1LC3C siRNA	Revvity	L-032399-01-0010
	ON-TARGETplus Human MAP1LC3B siRNA	Revvity	L-012846-00-0020
	ON-TARGETplus Non-targeting Pool	Revvity	D-001810-10
Cell lines	HAP1 parental control cell line	Revvity	C631
	Human ATG4B knockout cell line 8bp deletion	Revvity	HZGHC001241c010
	Human ATG7 Knockout cell line 2bp deletion	Revvity	HZGHC000302c022
	Human MAP1LC3B knockout cell line 7bp deletion	Revvity	HZGHC003241c005
	U-87 MG	ATCC	HTB-14
	KG-1	ATCC	CCL-246
	NCI-H1272	ATCC	CRL-5930
	NIH/3T3	ATCC	CRL-1658
	H-4-II-E	ATCC	CRL-1548
Compounds	AZD2014	MedChemExpress	1009298-59-2
	Hydroxychloroquine	Sigma	H0915
	Bafilomycin A1	Selleckchem	S1413
	ULK-101	Selleckchem	S8793
Antibodies	Anti-LC3B antibody produced in rabbit	Sigma	L7543
	Direct-Blot™ HRP anti-GAPDH Antibody	BioLegend	607904
	Goat anti-Rabbit IgG (H+L) Cross-Adsorbed Secondary Antibody, HRP	Invitrogen	G21234

References

Agrotis, A. et al., Redundancy of human ATG4 protease isoforms in autophagy and LC3/GABARAP processing revealed in cells. Autophagy. 2019 Jun;15(6):976-997. doi: 10.1080/15548627.2019.1569925

Bensalem, J. et al., Inhibiting mTOR activity using AZD2014 increases autophagy in the mouse cerebral cortex. Neuropharmacology. 2021 Jun 1:190:108541. doi: 10.1016/j.neuropharm.2021.108541

Bestion, E. et al., Update on autophagy inhibitors in Cancer: opening up to a therapeutic combination with immune checkpoint inhibitors. Cells. 2023 Jun 23;12(13):1702. doi: 10.3390/cells12131702

Debnath, J. et al., Autophagy and autophagy-related pathways in cancer. Nat Rev Mol Cell Biol. 2023 Aug;24(8):560-575. doi: 10.1038/s41580-023-00585-z

Feng, Y. et al., The machinery of macroautophagy. Cell Res. 2014 Jan;24(1):24-41. doi: 10.1038/cr.2013.168

He, C. et al., Regulation mechanisms and signaling pathways of autophagy. Annu Rev Genet. 2009:43:67-93. doi: 10.1146/annurev-genet-102808-114910

Kabeya, Y. et al., LC3, a mammalian homologue of yeast Apg8p, is localized in autophagosome membranes after processing. EMBO J. 2000 Nov 1;19(21):5720-8. doi: 10.1093/emboj/19.21.5720

Klionsky, D.J. et al., Guidelines for the use and interpretation of assays for monitoring autophagy (4th edition). Autophagy. 2021 Jan;17(1):1-382. doi: 10.1080/15548627.2020.1797280

Klionsky, D.J. et al., Autophagy in major human diseases. EMBO J. 2021 Oct 1;40(19):e108863. doi: 10.15252/embj.2021108863

Levine, B. et al., Autophagy in the pathogenesis of disease. Cell. 2008 Jan 11;132(1):27-42. doi: 10.1016/j.cell.2007.12.018

Martin, K.R. et al., A Potent and Selective ULK1 Inhibitor Suppresses Autophagy and Sensitizes Cancer Cells to Nutrient Stress. iScience. 2018 Oct 26:8:74-84. doi: 10.1016/j.isci.2018.09.012

Mizushima, N. et al., How to interpret LC3 immunoblotting. Autophagy. 2007 Nov-Dec ;3(6):542-5. doi: 10.4161/auto.4600

Mizushima, N. et al., Methods in mammalian autophagy research. Cell. 2010 Feb 5;140(3):313-26. doi: 10.1016/j.cell.2010.01.028

Mizushima, N. et al., The Role of Atg Proteins in Autophagosome Formation. Annu Rev Cell Dev Biol. 2011:27:107-32. doi: 10.1146/annurev-cellbio-092910-154005

Morel, E. et al., Autophagy: A Druggable Process. Annu Rev Pharmacol Toxicol. 2017 Jan 6:57:375-398. doi: 10.1146/annurev-pharmtox-010716-104936

Rebecca, V.W. et al., PPT1 Promotes Tumor Growth and Is the Molecular Target of Chloroquine Derivatives in Cancer. Cancer Discov. 2019 Feb;9(2):220-229. doi: 10.1158/2159-8290.CD-18-0706

Russell, R.C. et al., ULK1 induces autophagy by phosphorylating Beclin-1 and activating VPS34 lipid kinase. Nat Cell Biol. 2013 Jul;15(7):741-50. doi: 10.1038/ncb2757

Wang, W. et al., The carboxyl-terminal amino acids render pro-human LC3B migration similar to lipidated LC3B in SDS-PAGE. PLoS One. 2013 Sep 10;8(9):e74222. doi: 10.1371/journal.pone.0074222

Yamamoto, A. et al., Bafilomycin A1 prevents maturation of autophagic vacuoles by inhibiting fusion between autophagosomes and lysosomes in rat hepatoma cell line, H-4-II-E cells. Cell Struct Funct. 1998 Feb;23(1):33-42. doi: 10.1247/csf.23.33

Yang, Z. and Klionsky, D., Mammalian autophagy: core molecular machinery and signaling regulation. Curr Opin Cell Biol. 2010 Apr;22(2):124-31. doi: 10.1016/j.ceb.2009.11.014